Astrophysical Jets, STScI Symposium Series, **6**, ed. D. Burgarella, M. Livio, and C. O'Dea (Cambridge U. Press), pp. 73–94 (1993)

COMPACT EXTRAGALACTIC RADIO JETS

Alan P. Marscher
Department of Astronomy, Boston University
725 Commonwealth Ave.
Boston, MA 02215
USA

Abstract. Parsec-scale radio jets in radio-loud AGN connect the central region with the more extended jet and lobes. The sizescales of these compact jets are sufficiently small that the brightness, spectrum, polarization, and structure are observed to vary in most sources. The morphology typically consists of a very compact "core" from which protrudes a one-sided jet defined by a series of knots of emission. While some of these knots in a few sources are stationary, most are found to move outward along the jet at apparently superluminal speeds. The radio core is probably much larger than the region where the jet originates (the "base" of the jet). There is most likely an "inner jet" that extends from the base to the radio core yet is too small and opaque to be detected in VLBI images. Multifrequency monitoring observations from radio to γ-ray frequencies provide the best opportunity to explore the nature of this inner jet.

1. INTRODUCTION

The beautiful images of extragalactic radio jets obtained with the VLA (see Laing's paper in these proceedings) demonstrate that enormous amounts of energy in exotic forms are transported from the nuclei of radio galaxies and quasars to interstellar and intergalactic space. These beams of highly relativistic particles and magnetic field have remarkably narrow opening angles of only a few degrees. At milliarcsecond resolution, using VLBI, we find parsec-scale jets just as highly collimated, with features that not only move outward, but do so at speeds that appear to exceed that of light.

It is therefore apparent that something deep within the nucleus of the active galaxy generates relativistic, magnetized plasma, directs the plasma into an outward flow, and focuses the flow into a narrow cone. The main goal of studying compact jets is to determine how the plasma is energized, accelerated to relativistic flow speeds, and collimated into a thin jet. It is hoped that an understanding of these

processes will also shed light on the nature of the central engine that powers the nuclear activity in the galaxy or quasar.

There are two basic observational methods for studying compact jets. The first is direct imaging using VLBI. The second is to follow time variations in flux density and polarization at different wavebands. These two techniques are combined when one uses VLBI to monitor structural changes with time.

Fourteen years ago, Blandford & Rees (1978) proposed that variable extragalactic radio sources can be explained by relativistic jets, defined as collimated, gas dynamical flows containing collisionless relativistic plasmas threaded by a dynamically unimportant magnetic field and moving at bulk velocities close to the speed of light. Later that year, Readhead et al. (1978) published VLBI images using new hybrid mapping techniques which improved the dynamic range and fidelity considerably. These maps revealed that the compact radio sources observed consist of a compact "core" plus a one-sided series of knots that trace out a jet, thereby supporting the relativistic jet model. This model survives to the present day and has received support from a number observations that would be difficult to interpret in other ways.

In what follows, I will review the observations of compact extragalactic jets, relating the data to the relativistic jet scenario wherever applicable. I will also discuss speculative models that connect the jets on the scales observed with VLBI to the region immediately surrounding the central engine, whose main influence on the nonthermal source is limited to scales roughly two orders of magnitude smaller than can be directly imaged. Finally, I will indicate how further observations, especially multiwavelength monitoring, can test such models.

2. VLBI OBSERVATIONS OF COMPACT JETS

The basic observed structure of a compact radio jet consists of a "core" at one end with a series of knots extending more or less in the direction of the extended, kiloparsec-scale jet (although not all sources possess detectable large-scale jets). The knots tend to become more diffuse the farther they are from the core. In most sources, they separate from the core with apparent speeds that are superluminal. (The derivation of the velocity assumes that the distance to the quasar can be established using the Hubble Law.) In some sources, the knots trace out an essentially linear jet, whereas in other objects the jets are twisted. Typically, the compact jets either point directly toward the extended structure or curve toward that structure. Figure 1 shows an example of a straight compact jet, while the jet in Figure 2 exhibits pronounced twists.

Compact extragalactic radio sources do not always follow the core-jet morphology (Pearson & Readhead 1988). Of particular interest are the compact steep-spectrum and gigahertz-peaked spectrum sources, which typically have either complex compact structure or appear to be miniature versions of extended double-lobed radio sources. Some or all of the more complex sources could be either disturbed jets (for example, those that interact strongly with an external medium) or jets observed directly down the axis such that the full complexity of the microstructure of the jet is apparent. In this review I will discuss the more well-behaved core-jet sources, since these are more readily compared with current theoretical models.

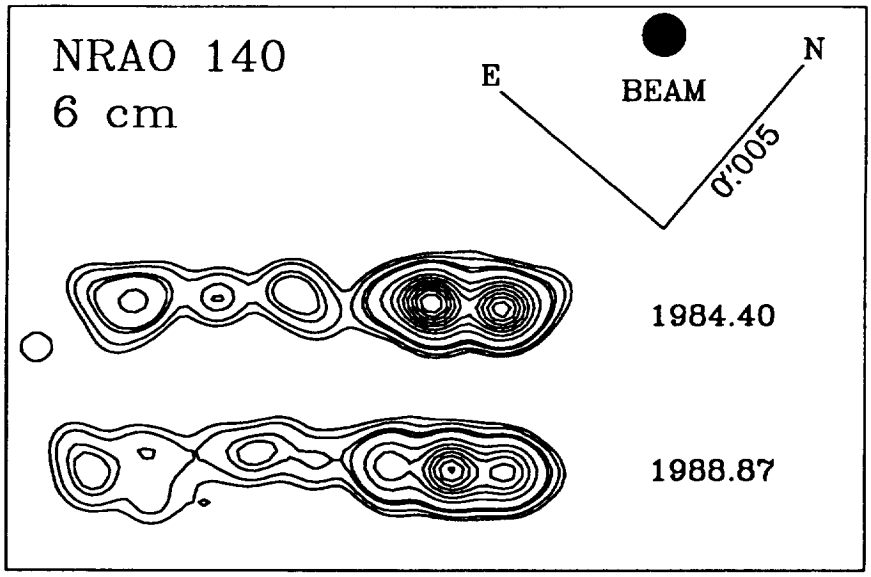

Figure 1. *VLBI image of the core-jet quasar NRAO 140 at a wavelength of 6 cm at two epochs. Contours are 2, 3, 5, 10, 20, 30, 40, 50, 60, 70, 80, and 90 percent of the 1984.40 peak of* 3.2×10^{10} *K (= 0.65 Jy beam*$^{-1}$*). Motion of the knots relative to the core (at the right-hand end of the jet), corresponding to an apparent speed of* $\sim 6.5c$ *($H_0 = 100$, $q_0 = 0.5$), can be seen. From observations obtained by the author.*

The parsec-scale core (not to be confused with the "core" seen on VLA images, which includes the entire compact emission region) is usually unresolved by Earth-based VLBI at centimeter wavelengths. Its spectrum is flat or inverted such that the core emission tends to dominate over that of the other components at frequencies higher than 30–100 GHz in most sources. It is not clear whether the core itself is highly variable, since during the early stages of a flare a new knot, if formed, is too close to the core to be distinguished from it using Earth-based VLBI. Hence, the core could be rather stable with variations occurring mainly in newly created knots. Space-based VLBI might be able to resolve the issue.

The most promising technique for studying the structure of the compact core is VLBI imaging at high frequencies. Recent progress has been made at 44 GHz, at which relatively high dynamic-range maps have been made of strong sources (e.g., Krichbaum & Witzel 1992). These images show "more of the same" in the sense that the structures are still core-jets, although in 3C 84 the position angles of the knots are quite time variable, indicating some interesting complexity. At 100 GHz the structures are still core-jets, with the suggestive result that a strong knot in 3C 273 detected in 1988 appeared to be significantly elongated perpendicular to the jet axis, suggestive of a thin shock wave (Bååth et al. 1992). It will be of great interest to extend these high-frequency VLBI observations to 230 GHz, which lies above the turnover frequency of the core in some strong sources. The images should therefore reveal the true structure of the core region, unimpeded by optical depth effects.

The knots in core-jet sources tend to become progressively more extended as they move away from the core. Observationally, it is the knots that define the compact jet, although Reid et al. (1989) find that the compact jet in M 87 is

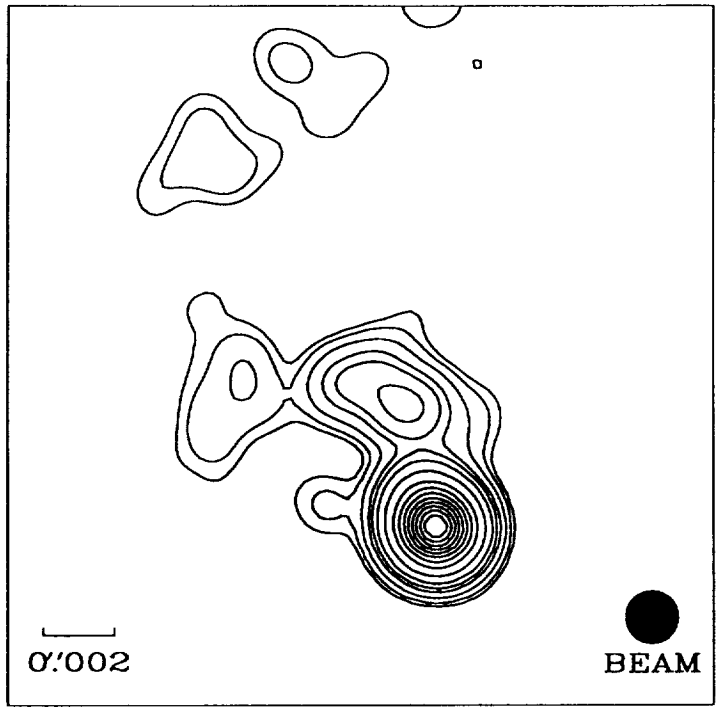

Figure 2. *VLBI image at λ = 6 cm of the twisted compact jet of the quasar 1156+295, observed in November 1988 (McHardy et al. 1990). The contour levels are 0.3, 0.5, 1, 2, 3, 5, 10, 20, ..., 90% of the peak brightness of 1.2 Jy beam^{-1}. An arcsecond-scale jet is also present, extending along position angle $-19°$.*

continuous when observed at very high dynamic range. In the quasar 3C 345, Biretta, Moore, & Cohen (1986) measure an opening half-angle (as projected on the sky) of 13°, while in the quasar NRAO 140 (see Fig. 1), Marscher (1988) measures 6°. If the jets are pointing in our direction, the true opening angles are considerably smaller (see § 3 below). The morphology of individual knots does not seem to follow any pattern, although the resolution and dynamic range of VLBI images are typically insufficient to explore the structure of each knot in detail. The few good spectral dissections made with multifrequency VLBI (e.g., Marscher 1988; Unwin et al. 1985) reveal that individual knots have spectra which roughly correspond to that expected from a uniform, self-absorbed synchrotron source. The turnover frequencies tend to be lower the farther the components are down the jet. In contrast, the core has a flatter spectrum below the turnover, with a power-law slope of 0.5 to 1.

Compact jets are overwhelmingly one-sided. For example, the jet:counterjet brightness ratio is observed to exceed 1600 in the case of 3C 345 (Rantakyrö et al. 1992). Under the standard relativistic jet model (see § 4 below), this upper limit provides a lower limit to the Doppler beaming factor and hence to the Lorentz factor and orientation angle of the jet. A very small number of (weak) compact jets appear to be two-sided (e.g., Venturi et al. 1993), although one must take care to observe

at a sufficiently high frequency that a downstream knot is not mistaken for the core and the core for a counterjet knot.

The knot:inter-knot ratio is not so easily determined, yet is an important parameter since it measures the enhancement to the emissivity caused by the knot, which is directly related to the physics of knot formation. In the 1984 image of the quasar NRAO 140 at $\lambda = 6$ cm shown in Figure 1, this ratio appears to be as large as 40 downstream of the brightest knot. The brightness of the ambient jet is, however, difficult to determine from this and most other existing VLBI images, since the ambient emission is more extended than the knots and hence can be resolved out by observations that do not include a sufficient number of short baselines. The VLBA will improve this situation significantly.

The flux density per unit length along the jet is observed to decline monotonically with distance from the core, save for an occasional abnormally bright downstream knot. In the cases of 3C 120 (Walker, Benson, & Unwin 1987a) and 3C 345 (Unwin & Wehrle 1992), the fall-off is described well by a power law of slope -1.3. In the case of 3C 120, the decrease in brightness follows this law over five orders of magnitude in distance from the core, and the spectral index of the jet emission remains roughly constant at a value $\alpha = -0.65$ (flux density $F_\nu \propto \nu^\alpha$).

The superluminal proper motions (measured relative to the core) of the knots are typically less than about $10c$ ($H_0 = 100$ km s^{-1} Mpc^{-1} and $q_0 = 0$ assumed) (Wehrle et al. 1992), although higher speeds are occasionally reported. Within a single source, the proper motions from one component to the next (referred to the same distance from the core) are similar in some documented cases (3C 273: Unwin 1990); 3C 120: Walker, Benson, & Unwin 1987b; NRAO 140: see Fig. 1), although in other cases (one component in 3C 120: Walker et al.1987b; 3C 345: Biretta, Moore, & Cohen 1986, Tang et al. 1990) substantial differences have been measured. It is interesting in the two cases of 3C 120 and 3C 345 that several recently appearing components are measured to have similar velocities, whereas older components have significantly different speeds. The superluminal speed in a jet may therefore be stable over a number of years before changing. In the case of 3C 345, components very close to the core (as seen on high-frequency VLBI maps) are observed to have curved trajectories with accelerating proper motions (Biretta, Moore, & Cohen 1986). In addition, the knots do not seem to follow identical trajectories as they separate from the core (Zensus 1990). Farther than ~ 0.5 millarcseconds from the core, however, the speed of a given knot is usually constant within the observational error. In some sources, such as 4C 39.25 (Shaffer et al. 1987), one or more components are superluminal while others are stationary relative to the core. In other sources, extremely rapid changes in the structure indicate that the time sampling is too sparse to determine systematic trends (e.g., 2134+004; Pauliny-Toth et al. 1990). In the case of 3C 345, Bartel et al. (1986) have verified that the core is stationary and the knots moving. (Normally, VLBI observations do not measure absolute phases and therefore do not yield absolute positions on the sky.)

As mentioned above, there is substantial curvature observed both within the compact jets and between the parsec-scale and kiloparsec-scale jets. In the case of 3C 120, the jet is found to curve continuously between the two scales (Walker, Benson, & Unwin 1987a,b). In their survey of strong sources, Pearson & Readhead (1988) found that, at a moderate significance level, the difference between small- and large-scale position angle tends to cluster near 0° and 90°. Conway (1993) finds that this can be explained within the context of the relativistic jet model if the jet

is presumed to execute a helical twist. The differential Doppler boosting caused by the changing orientation of the jet then causes the preference toward 90° if the jet lies nearly along the line of sight, while 0° is favored for other orientations or if the intrinsic curvature is low.

The polarization structure of compact jets has recently been explored by the group at Brandeis University (Roberts et al. 1990; Gabuzda et al. 1992). In general, they find that the cores tend to have very low polarization, perhaps indicating that differential Faraday rotation (Faraday depolarization) occurs. The knots, on the other hand, tend to be strongly polarized. Curiously, the polarization position angle tends to be nearly parallel to the jet in BL Lac objects (magnetic field direction perpendicular to the jet axis), and perpendicular in quasars. This strong dichotomy stands in contrast to the basic similarities in morphology of the compact jets in the two classes. On the other hand, the compact jets in BL Lac objects tend to be shorter (i.e., have steeper intensity gradients) and radio-bright BL Lac objects tend to have stronger X-ray emission than do quasars. The overall polarization characteristics of compact jets — substantial linear polarization and very low circular polarization — plus the tendency of observed brightness temperatures to obey the 10^{12} K inverse Compton limit, indicate that the emission process in compact jets is incoherent synchrotron radiation.

Although most VLBI observations have insufficient dynamic range to detect anything but the basic structure, some high dynamic-range images have shown considerable complexity, similar to that found on arcsecond scales. For example, the compact jet of M 87 displays filamentary structure (Biretta, these proceedings), while 3C 345 shows wiggles at the jet boundary, edge-brightening over a portion of the jet, and a sharp edge on the inner side of a broad component oriented perpendicular to the jet axis, suggestive of a reverse shock wave (Unwin & Wehrle 1992). These all correspond to features expected in fluid jets (e.g., Norman, these proceedings).

3. VARIABILITY OF THE FLUX DENSITY AND POLARIZATION OF EXTRAGALACTIC SOURCES

It seems to be a property of nature that objects composed of plasma vary on timescales as short as allowed by the laws of physics. The most basic limitation on timescale is the light-crossing time. Most compact extragalactic objects seem to vary by tens or hundreds of percent even faster than this, and those that do so are referred to as "blazars." The term includes both quasars and BL Lac objects.

The vast assortment of observations of spectral variability of blazars have revealed a diverse range in characteristic behavior. There are many similarities and differences both among sources and among flares within the same source. At the risk of oversimplifying, I list the major properties of spectral variability that I feel best exemplify the nature of the phenomenon, while recognizing that there are exceptions to these patterns.

(i) Flares usually begin at high frequencies, then propagate to lower frequencies. Some flares, however, develop simultaneously over a wide range of frequencies before propagating to lower frequencies, and still others do not seem to move to lower frequencies at all. Some events begin at optical-infrared wavelengths, while others begin at submillimeter, millimeter, or even centimeter wavelengths (see Epstein et

al. 1982; Aller et al. 1985).

(ii) The flaring emission usually rises abruptly, propagates to lower frequencies while maintaining essentially a constant amplitude, and then dies, sometimes gradually (as in AO 0235+164; O'Dell et al. 1988) and sometimes rapidly (as in 1156+295; McHardy et al. 1990).

(iii) Superposed on the flares, and sometimes on the "quiescent state," are mini-flares and/or rapid flickering; viz., the light curves are not smooth.

(iv) To first order, the multi-waveband spectra connect smoothly from the radio to the infrared. However, when observed with sufficient frequency coverage, the spectra often show double peaks (Brown et al. 1989). The timescale of variability is shorter at the higher frequencies. The polarization behavior also tends to be much more erratic at these frequencies.

(v) In some sources, rapid flickering has been observed at the $\lesssim 10\%$ percent level at centimeter wavelengths by Heeschen et al. (1987), Quirrenbach et al. (1989), and Krichbaum, Quirrenbach, & Witzel (1992). The flickering occurs on the same timescales as found in the optical. In fact, in the BL Lac object 0716+714, the variations are quasi-periodic, with the same quasi-period (although not the same phase) at both radio and optical wavelengths over several "cycles" of the light curve (Quirrenbach et al. 1991).

The two most fundamental problems associated with the timescales of variability are superluminal flux variations (apparently correlated brightness changes in two or more regions separated by a distance $\gtrsim c\Delta t$) and brightness temperatures that exceed the inverse Compton limit of 10^{12} K derived by assuming that the size of the emitting region is less than $c\Delta t$. Cases of apparent superluminal flux variations have been reported by Mutel, Aller, & Phillips (1981), Pauliny-Toth et al. (1987), Götz et al. (1987), and Pauliny-Toth et al. (1990).

The highest brightness temperatures inferred from variability observations are derived for low-frequency variations on timescales of months at meter wavelengths (Cotton & Spangler 1982) and intraday variations at centimeter wavelengths (Qian et al. 1991). The most troublesome low-frequency fluctuations, however, are now thought to be caused by refractive interstellar scintillations rather than variations intrinsic to the source (Rickett, Coles, & Bourgois 1984). The highest brightness temperature inferred from the intraday variations is $\sim 2 \times 10^{18}$ K (Qian et al. 1991).

The polarization of a compact extragalactic radio source is typically even more highly variable than the flux density, with rapid swings in position angle — by as much as 180° — often observed (e.g., Aller et al. 1985; Qian et al. 1991; Sillanpää & Takalo 1992).

Variability observations of extragalactic sources with compact jets at X-ray and γ-ray wavelengths are not yet extensive. BL Lac objects tend to be highly variable at X-ray energies (e.g., Maraschi 1992) and tend to have steeper X-ray spectra than do quasars (Worrall & Wilkes 1990). In fact, the spectra of some BL Lac objects appear to be continuous from radio to X-ray frequencies, indicating a common emission mechanism — presumably synchrotron radiation — in the compact jet. Quasars are also variable at X-ray energies (e.g,, 3C 273: Tananbaum et al. 1979, Courvoisier et al. 1987; 3C 279: Makino et al. 1989; NRAO 140: Marscher 1988), although not many cases are well documented. The X-ray spectra of quasars are rather flat (Wilkes & Elvis 1987), too much so to be explained as continuations of the optical-uv emission.

The recent detections of a number of quasars and BL Lac objects containing

compact jets by the *Compton Observatory* at hard γ-ray energies demonstrate that a significant, in some cases dominant, fraction of the nonthermal luminosity is emitted at extremely high energies (Hartman et al. 1992 and various IAU Circulars). The γ-ray flux from the quasar 3C 279 was reported to be variable by a factor of three over a 4-month period and also to be significantly variable on a timescale of a few days (Kanbach et al. 1992). The BL Lac object Mk 421 has also been detected at TeV energies (1 TeV = 1.6 ergs = 2.4×10^{26} Hz!) (Weekes 1992).

The overall multifrequency variability of nonthermal sources has yet to be studied extensively, although monitoring campaigns are planned from radio to γ-ray frequencies in late 1992 and 1993. There are, however, a number of studies that have demonstrated that flares in nonthermal sources are often broadband in nature. A direct correspondence between X-ray and radio–infrared variability has been found in 3C 279 (Makino et al. 1989). In the case of BL Lac, Kawai et al. (1991) found that the X-ray flux was correlated with the submillimeter-wave flux. In NRAO 140, Marscher (1988) found a similar relationship between the X-ray flux and the flux of the radio core as measured with VLBI. Courvoisier et al. (1987), on the other hand, found little correspondence across wavebands in the variations of 3C 273, although the sampling rate was somewhat sparse.

Bregman et al. (1990) and Hufnagel & Bregman (1992) have analyzed in detail the variations occurring at radio, infrared, and optical frequencies in BL Lac and several other blazars. They find that there is no significant time delay between features in the optical and infrared light curves, but that there is a delay of about 1 year between the weakly correlated optical and radio variations. They also find that the optical variations can be characterized by a combination of shot noise and flicker, whereas the radio variations have power spectra similar to shot noise. The conclusion is that flickering is a high-frequency phenomenon in the sources studied, and that the radio emitting region is larger than, but connected to, the site of the optical emission.

4. THE RELATIVISTIC JET MODEL

The standard relativistic jet model used as the paradigm for interpreting observations of compact jets was first presented by Blandford & Rees (1978) and expanded upon by Blandford & Königl (1979), with certain aspects added later by Reynolds (1982), Marscher (1980), and Königl (1981). The visible portion of the jet, schematically drawn in Figure 3, is assumed to begin at some point R_0, beyond which it flows at a constant Lorentz factor Γ_j (speed $\beta_j c$), confined to a truncated cone of constant opening half-angle ϕ. The radial coordinate R is measured from the apex of this cone. Although it is not necessary for the cone to have a constant opening angle, this simple geometry conforms quite well to the available VLBI observations. If one further assumes that the jet is free (confined solely by its own inertia), it resembles a conic section of a spherical wind. The density therefore falls off as R^{-2}, while the component of the magnetic field parallel to the jet $B_\parallel \propto R^{-2}$ and the component transverse to the jet $B_\perp \propto R^{-1}$. The region near $R = R_0$ contains the highest density and magnetic field strength of the conic portion of the jet, and therefore appears as a stationary, bright feature even though plasma streams through it at a relativistic speed. In the model, this region is identified with the VLBI core. Although it is not clear whether the portion of the jet at radii $R < R_0$ is directly observable at

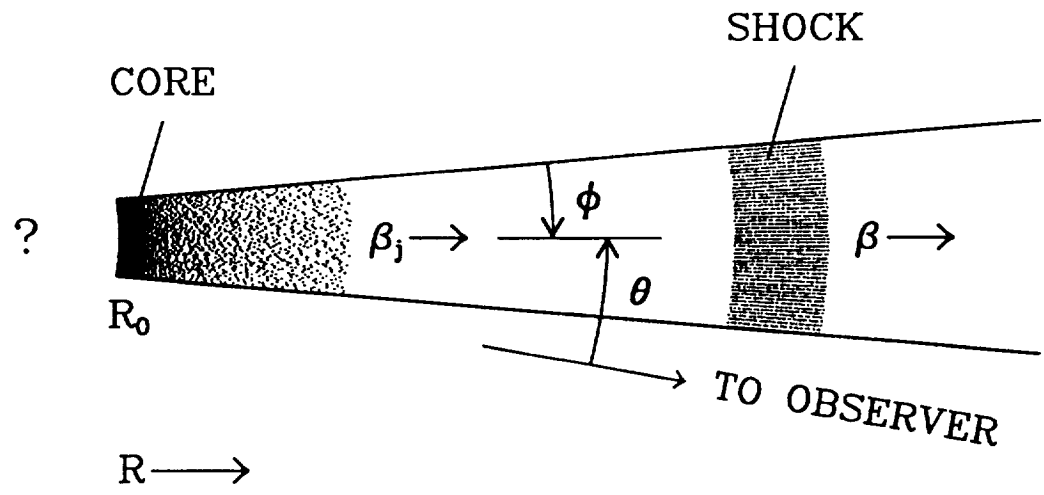

Figure 3. *Basic geometry of the relativistic jet model as viewed from a direction transverse to the axis. The vertical scale is expanded by a factor of a few for visual clarity.*

any waveband, it is important to explore possible observational signatures revealing the geometry and physical characteristics of this region, since it connects the jet with the central engine. The origin and and energization of the jet plasma and collimation and bulk acceleration of the jet flow also occur in this region. I return to this point in § 4 below.

The relativistic jet model relieves the major theoretical difficulties associated with blazars. Relativistic beaming of the emission toward the observer causes one to miscalculate the luminosity and photon density of the source. In order to derive these quantities, one needs to multiply the observed integrated flux F by $4\pi D_l^2$ to obtain the luminosity at the source, where D_l is the luminosity distance. However, if relativistic beaming occurs, the radiation is not emitted isotropically, and the timescales are contracted in the observer's frame. Therefore, one must multiply F by a factor δ^{-4} for a variable emission region moving within the jet, where $\delta \equiv [\Gamma(1 - \beta\cos\theta)]^{-1}$ and θ is the angle between the jet axis and the line of sight. The Doppler factor δ ranges from $(1+\beta)\Gamma$ for $\theta = 0$, to Γ for $\theta = \sin^{-1}(1/\Gamma)$, to Γ^{-1} for $\theta = \pi/2$. Any given flux-limited survey tends to be dominated by beamed sources, so one has no problem with statistics as long as there is a sufficient supply of "parent" objects that have low apparent luminosities because most of their radiation is beamed away from us. Since the actual luminosities of sources with jets beamed toward us are much lower than previously inferred, the enormous energy requirements and overprediction of high-energy inverse Compton photons are greatly diminished.

Since we have yet to understand how a relativistic jet is focused and accelerated, we cannot yet obtain a firm theoretical upper limit to the Lorentz factor of the jet. However, if the jet is accelerated near the putative massive black hole, Compton drag should limit the Lorentz factor to $\Gamma_j \lesssim 10$, and there are other arguments that lead to a similar constraint (Phinney 1987). One can use the measured angular size, turnover frequency, and flux density to derive the magnetic field and energy

density in relativistic electrons of a source. When this is done for a typical compact component in a blazar without correcting for relativistic beaming, one finds that the energetics are dominated by the relativistic electrons (see Burbidge, Jones, & O'Dell 1974; Marscher & Broderick 1985). If one assumes that the component is moving relativistically with a Doppler factor δ, this imbalance is lessened and the total energy requirement is correspondingly diminished. But once the Lorentz factor exceeds about 10, the magnetic field begins to dominate and the energy requirements become extremely high. The other consequence of very high Lorentz factors is that the more highly beamed blazars are, the greater is the required number of unfavorably beamed parent objects. This also restricts the *typical* value of Γ to be $\lesssim 10$, although *a few* extraordinary objects could have higher values. The "critical" value $\Gamma \sim 10$ is a rough one, but the arguments are general. It is interesting that the observed superluminal speeds seem to obey this limit.

The true opening half-angle ϕ of the jet is related to the observed angle ϕ_{obs}, projected on the sky, by the relation $\phi \approx \phi_{obs} \tan\theta$ in the small-angle limit. Since the angle of the jet axis relative to the line of sight θ can be estimated from the observed superluminal motion (by minimizing the bulk Lorentz factor Γ), it is possible to derive the value of ϕ. For NRAO 140, Marscher (1988) obtains $\phi \approx 1\overset{\circ}{.}5$, while for 3C 345 (Unwin and Wehrle 1992), one can calculate $\phi \approx 1\overset{\circ}{.}6$. The relativistic jet model therefore requires that the jets be extremely well collimated.

Blandford & Königl (1979) proposed that disturbances in the jet flow cause shocks to form and propagate down the jet. They associated these shocks with the knots observed to move at apparent superluminal speeds in VLBI images of compact extragalactic jets. Jones (1982), Marscher & Gear (1985), and Hughes, Aller, & Aller (1985) subsequently showed that such shocks could reproduce quite well many of the detailed characteristics of the structural, spectral, and polarization variability of blazars.

Probably the greatest success of the detailed shock-in-jet models is their reproduction of complex observed multifrequency spectral and polarization variations while obeying the constraints of a specific physical scheme. This success led Marscher, Gear, & Travis (1992) to include the complicating effects of bending of the jet and turbulence in the jet plasma.

VLBI and VLA observations of jets show that they often bend considerably. For relativistic jets, the small angle of the jet axis to the line-of-sight amplifies the bending angle. Even so, bends of at least several degrees are required by the observations. Although it is not necessarily true that the jet axis itself bends, this is the most straightforward interpretation of the observations. Hardee (1990) has shown that macroscopic fluid instabilities can cause a jet to bend. Curvature in a relativistic jet causes variations in Doppler boosting and proper motion. These effects lead to systematic changes in the observed brightness and apparent superluminal motion of a compact source.

The observational consequences of variations in the inclination angle of the jet θ are described by Marscher (1990) and Marscher, Gear, & Travis (1992). The Doppler boosting of the flux density can change by a factor of 2 or so even if the jet bends by only a few degrees. This is accompanied by a noticeable change in the apparent superluminal speed if θ changes from $\lesssim 15^\circ/\Gamma$ to larger angles (or *vice versa*), or by only a modest change in v_{app} if θ remains in the $30^\circ/\Gamma$ to $110^\circ/\Gamma$ range.

The evolution of the spectrum of a shock moving down a twisted jet has been considered by Marscher, Gear, & Travis (1992). The several possible

patterns include a rise in flux density as the self-absorption turnover frequency remains essentially constant or decreases. This behavior has been observed in the centimeter-wave outbursts such as that in the source 1921-29 in 1979 (Dent and Balonek 1980) and that in 1156+295 in 1984–86 (McHardy et al. 1990). While this behavior can be reproduced at higher frequencies if inverse Compton losses are important (Marscher & Gear 1985), it is difficult to conceive of an alternative mechanism for doing so at centimeter wavelengths since changes in other physical parameters that cause the flux density to increase should cause the turnover frequency to increase as well.

Marscher et al. (1991) and Alberdi et al. (1993) have interpreted the peculiar superluminal quasar 4C 39.25 in terms of a bending jet. The model interprets the stationary features in the compact jet as points where the angle to the line of sight is minimized: at such points the Doppler beaming is enhanced but the apparent transverse motion is greatly diminished. The evolution of the multifrequency light curve follows that expected according to the model. In addition, the polarization observations indicate that the magnetic field is oriented transverse to the jet axis, as expected for a strong shock wave in a turbulent jet, and contrary to the trend for quasars determined by Roberts et al. (1990).

The Reynolds number in a relativistic jet is expected to be extremely high, so the plasma in the jet should be quite turbulent. The effect that this has on the time variability depends on the amplitude and power spectrum of the turbulence as well as on the thickness of the shocked emission region. Marscher & Travis (1991) and Marscher, Gear, & Travis (1992) present numerical simulations of a shock propagating down a jet whose plasma is hydromagnetically turbulent. As the disturbance propagates down the jet, it brightens at sites where it encounters density and/or magnetic field enhancements and fades where it encounters diminishments. It is mainly the magnetic field fluctuations that amplify or reduce the flux density at a given location in the shock. Especially effective are changes in the direction of the magnetic vector, since the observed synchrotron radiation depends strongly on the orientation of the magnetic field relative to the observer.

The shock should have a frequency-dependent dimension along the jet axis at high frequencies, since the high-energy electrons radiating at these frequencies suffer significant synchrotron and (perhaps) inverse Compton losses. The highest amplitude variability is caused by the overall evolution of the shock wave and is nearly simultaneous over all optically thin portions of the spectrum, which for major flares typically includes optical, infrared, submillimeter, and perhaps millimeter wavelengths. If the disturbance is strong enough (but not so strong that radiative losses completely snuff it out), the flare propagates toward longer wavelengths, peaking as the emission at that wavelength becomes optically thin, viz. later at longer wavelengths. Superposed on this long-term (timescales of months, typically) trend are substantial flares occurring on timescales governed by the decorrelation length scale of the turbulence. Minor fluctuations ("flickering") superposed on the more pronounced flux density variations can occur over even shorter timescales as the shock encounters eddies of dimensions similar to the width of the emission region behind the shock front at that frequency, $x(\nu)$. The variability timescale is found to be as short as $\sim x(\nu)/(\gamma c)$, so very rapid variability, much faster than $\sim R/c$, is possible if the shock is very thin ($x \ll R\phi$) The timescales of these minor variations are shorter, and the amplitudes larger, at the higher frequencies corresponding to smaller values of $x(\nu)$. Figure 4 illustrates the general nature of the numerically

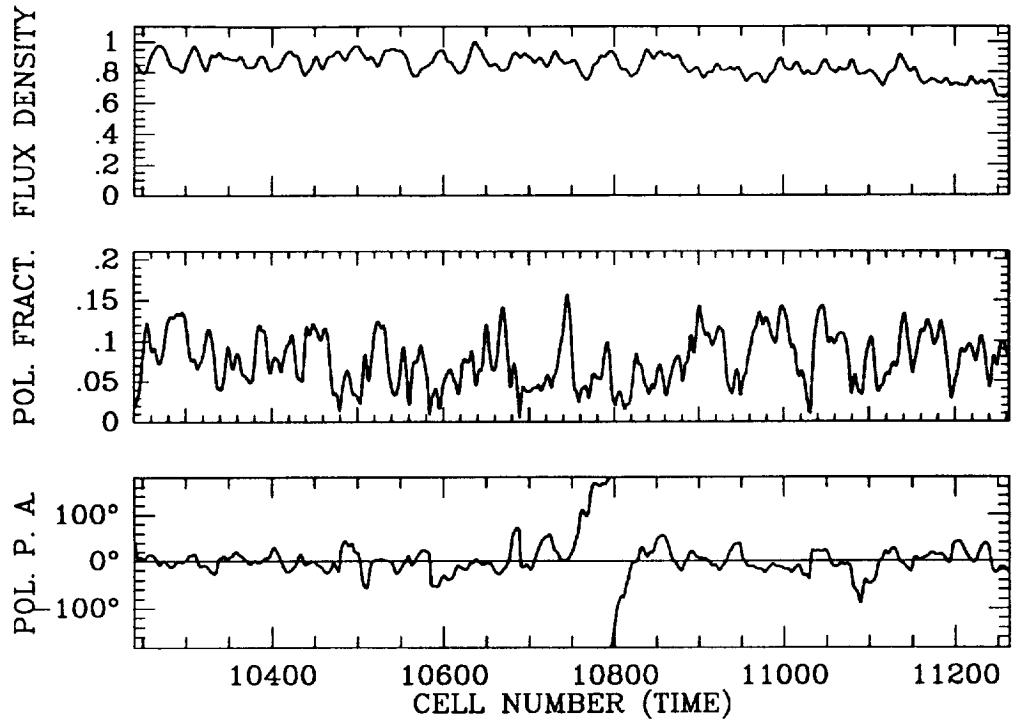

Figure 4. *Total flux density (normalized), polarization fraction, and polarization position angle "light curves" corresponding to a numerical simulation of a thin shock propagating through a turbulent jet. The gradual decline in flux density is caused by the overall evolution of the shock emission, while the rapid flickering occurs as the shock encounters turbulent fluctuations in magnetic field and density. The mean magnetic field is parallel to the jet axis (perpendicular to the shock front); superposed on this is a random component with magnitude equal to 80% of the mean field. The density fluctuations correspond to 10% of the mean value. From Marscher, Gear, & Travis (1992).*

generated flickering of the flux density and polarization. Note the high amplitude of the polarization variations, including a position angle swing of over 180° that is nothing more than a "random walk" as the shock encounters turbulent cells with randomly oriented magnetic field. Figure 5 shows the frequency dependence of the light curves. The lower frequency light curves are much smoother than those at higher frequencies, which exhibit considerable flickering.

The turbulent fluctuations can occur far downstream of the compact core of the source. Shocks in turbulent jets are therefore good candidates for explaining much of the "flickering" of radio sources (Heeschen et al. 1987; Quirrenbach et al. 1989). However, it is not clear how shocks thin enough to cause variations on timescales $\sim$ 1 day can occur at centimeter wavelengths, since radiative losses should be negligible. If such thin shocks are possible, the flickering radio emission could be synchrotron radiation from shocks moving through turbulence, while the similar optical variations observed in 0716+714 (Quirrenbach et al. 1991) could be inverse Compton scattered radiation generated inside the flickering radio

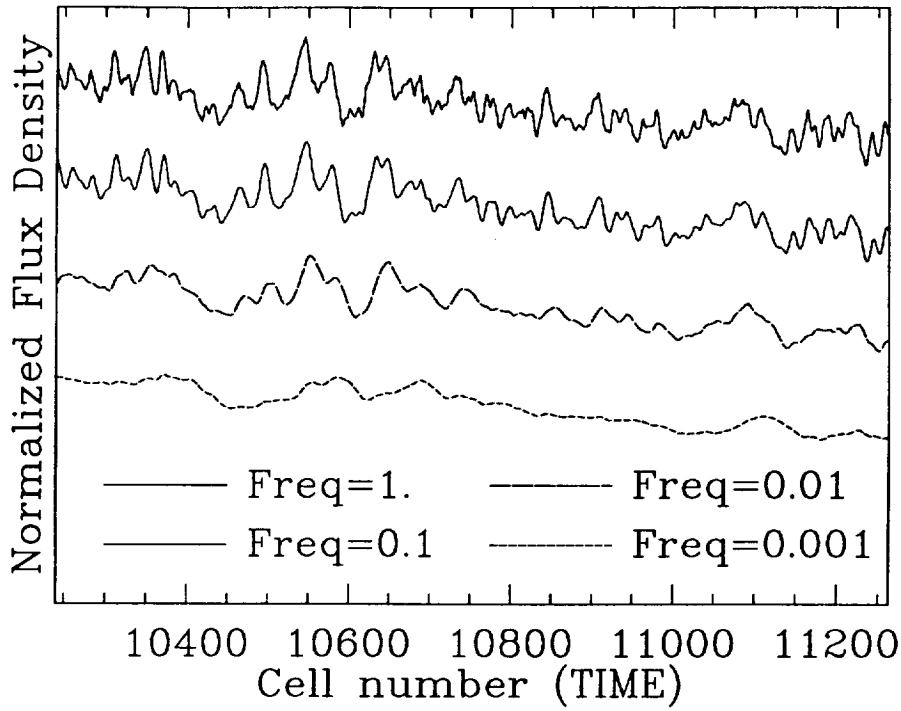

Figure 5. *Total flux density (normalized) "light curves" at four normalized frequencies corresponding to a numerical simulation of a thin shock propagating through a turbulent jet (as in Fig. 4 but corresponding to a different run). Note that the light curves become smoother toward lower frequencies. From Marscher & Travis (1992).*

synchrotron component. I have explored this in a previous paper (Marscher 1992), where I found that a thin shock in a turbulent jet can indeed produce intraday variations similar to those observed, but only if the jet is pointing directly along the line of sight. The implied brightness temperature of 2×10^{18} derived by Qian et al. (1991) should represent an extreme case, since it can be explained only by the most favorable orientation of the jet relative to the observer. Also, while turbulence can provide quasi-periodic phenomena over several cycles, truly periodic intraday variations cannot be accommodated. Such periodicities would probably require coherent emission mechanisms, which seem unlikely given that the polarization properties of the intraday variables (substantial linear polarization, very low circular polarization) are identical to those observed in garden-variety incoherent synchrotron sources.

The radio-infrared synchrotron flare caused by a shock in a jet should be accompanied by a self-Compton X-ray and γ-ray flare. Since the self-Compton flux density is proportional to the synchrotron photon density as well as the density of relativistic electrons, both of which increase during an outburst, the high-energy flare should be more pronounced than the synchrotron flare, after subtraction of the "quiescent" emission. Because of the close connection observed between the optically thin synchrotron emission and the X-ray emission in blazars, most authors

consider self-Compton scattering to be the primary X-ray emission mechanism in all such sources except for those BL Lac objects with steep X-ray spectra. For the latter sources, synchrotron emission appears to be the dominant mechanism. Since the extragalactic sources detected at hard γ-ray energies by the *Compton Observatory* thus far all contain compact nonthermal jets, it is clear that the γ rays are intimately connected with the lower frequency synchrotron emission. Since the γ-ray spectra are obviously not merely continuations of the lower frequency synchrotron spectra, and since γ-ray synchrotron emission would require extraordinarily high energy electrons and strong magnetic fields, processes such as inverse Compton emission or proton decays are more likely mechanisms. The hard γ-ray emission almost surely arises well outside the region immediately surrounding the central engine, since otherwise photon-photon pair production would cause the γ rays to be absorbed (McBreen 1979). The γ rays therefore probably originate either near the VLBI core or deep within the "inner jet" that connects the radio jet with the central engine. The same can be said about the X-ray emitting region. The very short timescale of variability of the γ-ray emission from 3C 279 (Kanbach et al. 1992) implies that the inner jet may indeed be the source of the high-energy emission, as suggested by Maraschi, Ghisellini, & Celotti (1992). Since there is therefore hope that the inner jet may be observationally accessible, I now discuss it in some detail.

4. THE INNER JET

Several speculative models have been proposed to connect the inner jet with the radio jet observed with VLBI. Here I summarize the most popular ones and relate them to past and future observations.

As discussed by Begelman, Blandford, & Rees (1984), much of the collimation of the jet must occur close to the central engine, since external pressure gradients are insufficient to focus a flow to within an opening angle of 1° to 3°. The collimation most likely involves the twisting of magnetic fields caused by the differential rotation of the accretion disk (see Blandford's contribution to these proceedings). If there is only partial focusing, pressure gradients can do the rest. In this case, the internal energy of the relativistic plasma is converted to bulk flow energy as long as the jet is confined and the internal energy of the plasma significantly exceeds the rest mass energy. The geometry of such a jet is shown in the top panel of Figure 6. Another possibility, depicted in the bottom panel of the same figure, occurs if a magnetic dynamo mechanism generates a highly relativistic (Lorentz factors of 10^2 to 10^4) beam of electrons and positrons streaming along the polar magnetic field lines of the accretion disk (Lovelace 1976; Blandford & Znajek 1977). Phinney (1987) and Melia & Königl (1989) have shown that up-scattering of the uv photons emitting by the accretion disk decelerates the electron-positron stream to a terminal bulk Lorentz factor $\sim$ 10. The scattering, along with plasma instabilities, can also randomize the pitch angles such that the beam becomes a flowing plasma by this point, which corresponds to the core of the radio jet.

The radiation expected from an accelerating inner jet has been explored by Marscher (1980), Reynolds (1982), Ghisellini, Maraschi, & Treves (1985), Celotti, Maraschi, & Treves, and Maraschi, Ghisellini, & Celotti (1992). If the acceleration of the relativistic electrons occurs only in the region closest to the central engine, the synchrotron emission at uv, optical, and IR frequencies is confined to this region as

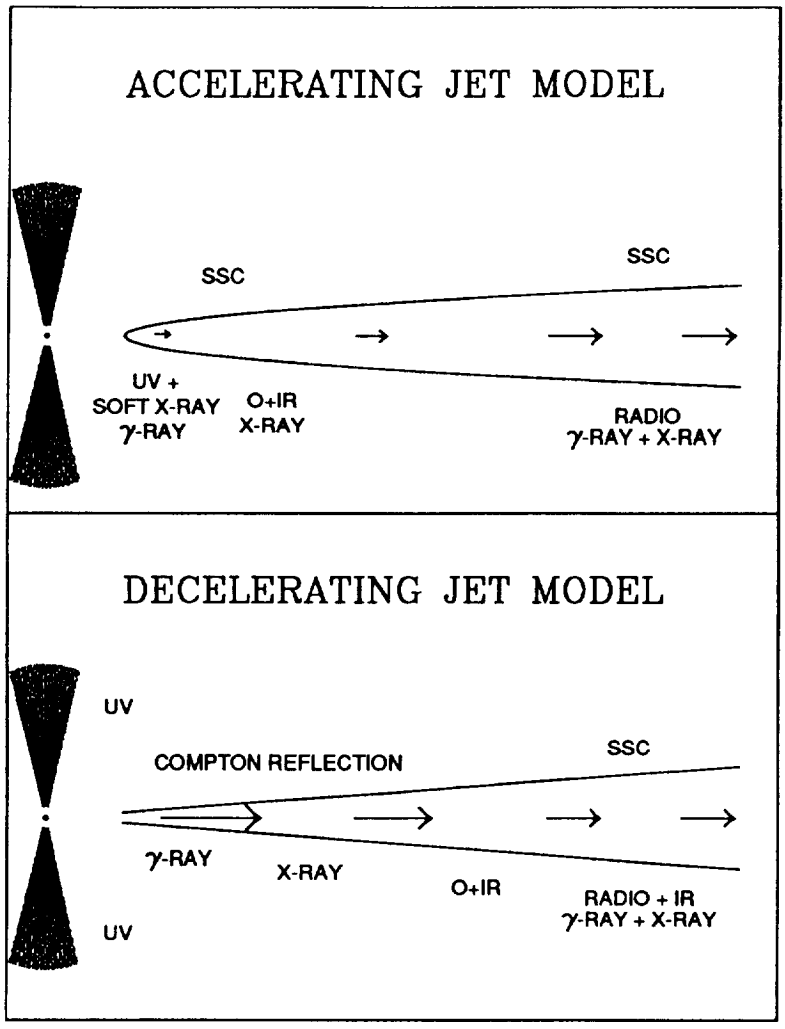

Figure 6. *Two basic models for the inner jet that connects the compact radio jet with the central engine, here depicted as a massive black hole with an accretion disk. Presumably, a second jet extends to the left of the central engine as well. The figures are schematic cross sections and not drawn to scale. The arrows inside the jet correspond to the magnitude of the bulk Lorentz factor of the jet flow on a logarithmic scale. The right-hand side of the jet corresponds to the left-hand side of the radio jet depicted in Fig. 3. The primary emission mechanism of each region is indicated above the jet, with "SSC" corresponding to synchrotron self-Compton emission. The main frequency bands of the nonthermal emission are indicated below the jet, with synchrotron or Compton reflection on top and self-Compton on bottom. Upper panel: Jet flow accelerates as internal energy is converted to bulk flow energy (e.g., Marscher 1980; Maraschi et al. 1992). Lower panel: A highly relativistic stream of electrons and positrons reflects ultraviolet radiation from the accretion disk, up-scattering the uv photons to X-ray and γ-ray energies. The interaction causes the beam to decelerate to a final Lorentz factor ~ 10 (Melia & Königl 1989; Phinney 1987).*

well, which is opaque to radio emission. Outside of this UVOIR region, the highest energy electrons emit only at lower frequencies, having suffered from radiative and adiabatic losses. However, if the inner jet does not open too abruptly, the maximum radio emission occurs where the Lorentz factor, and hence the Doppler boosting, is strongest. This region is then identified as the radio core, with the radio jet visible on the downstream side. Substantial self-Compton γ-ray and X-ray emission can occur either in the UVOIR region or the radio core (see Maraschi et al. 1992). In addition, (inverse) Compton relection of optical and uv photons from the accretion disk can take place in the UVOIR region, producing X-rays and γ rays (Dermer, Schlickeiser, & Mastichiadis 1992).

Begelman & Sikora (1987) and Melia & Königl (1989) have discussed Compton reflection of the optical and uv photon from the accretion disk off a highly relativistic stream of electrons. The process emits γ rays from the deepest part of the inner jet and X-rays somewhat downstream of this, with the nonthermal optical to radio emission occurring farther out. An interesting aspect of Compton reflection is that photons approaching a stream of electrons from behind are scattered primarily into a hollow cone of opening angle $\sim \Gamma$, so that the emission is quite low if one views directly down the axis of the jet (Melia & Königl 1989; Dermer et al. 1992). This conflicts with the model described in § 3 for the intraday flux variations in the BL Lac object 0716+714. The model requires that we view the jet directly down the axis. This implies that either the jet is bent through an angle $\sim \Gamma$ or the hard γ rays observed from this object (Michelson et al. 1992) do not arise from Compton reflection.

In both of these basic models the emission regions at different wavebands are connected but lie at different distances from the central engine. One can therefore potentially use multifrequency observations to discriminate among the models. Variations occurring in shocked regions near the radio core should have the characteristics described in § 3: simultaneous brightness and polarization fluctuations at higher frequencies and slightly time-delayed and less pronounced variations at lower frequencies (but still above the self-absorption turnover). For the two inner jet models, however, disturbances propagating down the jet are time-delayed at different wavebands, depending on the location of the primary emission region at each frequency. For example, in the decelerating jet model, uv flares should occur before γ-ray and X-ray flares, which should later lead into radio–infrared outbursts. It is also possible in the context of this model for the flare to be caused by an enhanced flow of electrons in the stream, in which case a γ-ray and X-ray flare would precede a radio–infrared outburst with no uv flare. In the specific accelerating jet model of Maraschi et al. (1992), the uv and γ-ray emission varies simultaneously, as does the IR and X-ray emission, but the latter fluctuations follow the former by a day or so, with the submillimeter outburst occurring later still. There are a number of other possible combinations, since precisely where the emission regions at each waveband lie depends on the details of the jet geometry and particle acceleration.

5. CONCLUSIONS

The relativistic jet paradigm seems to explain a wide range of characteristics observed in compact jets. This is remarkable given the relative simplicity of both the

geometry and physics assumed. Still, one has the impression from both numerical simulations of jet fluid dynamics and observations such as those of M 87 (see Biretta's contribution to these proceedings) that actual jets are much more complex than the basic model allows. I hope that the high dynamic range allowed by the VLBA and future simulations of jets with relativistic flow velocities will soon allow us to inject a larger dose of realism into the models. It is almost certainly true that we will find that some of our simplifying assumptions are woefully inadequate to the task of describing compact jets.

It is somewhat disappointing that the smallest observable features of the radio jets are much larger than the expected interaction scale between the central engine and the deepest regions of the plasma flow that emerges downstream as a well-collimated relativistic jet. Fortunately, it now appears that this "inner jet" region produces a high luminosity in X-rays and γ rays, and is therefore observationally accessible. Multifrequency monitoring of a few selected objects across all wavebands are now planned for late 1992 and 1993. Inspection of the data for correlated variability and time delays should reveal the relative location of the nonthermal emission at each waveband. This will allow us to infer the geometry and physics of the inner jet, which in turn should lead to a better understanding of the processes by which the jet is focused and accelerated. When combined with observations of the thermal emission from active galaxies, this information should allow us to develop a complete model of active galaxies, from the central engine to the jet and extended lobes.

The author's work on compact jets is supported in part by National Science Foundation grant AST-9116525 and NASA grants NAGW-1068 and NAG 5-1566.

REFERENCES

Alberdi, A., Marcaide, J.M., Marscher, A.P., Zhang, Y.F., Elósegui, P., Gómez, J.L., & Shaffer, D.B. 1993, ApJ, 402, in press

Aller, H.D., Aller, M.F., Latimer, G.E., & Hodge, P.A. 1985, ApJS, 59, 513

Bååth, L.B., et al. 1992, A&A, 257, 31

Bartel, N., Herring, T.A., Ratner, M.I., Shapiro, I.I., & Corey, B.E. 1986, Nature, 319, 733

Begelman, M.C., Blandford, R.D., & Rees, M.J. 1984, Rev. Mod. Phys., 56, 255

Begelman, M.C., & Sikora, M. 1987, ApJ, 322, 650

Biretta, J.A., Moore, R.L., & Cohen, M.H. 1986, ApJ, 308, 93

Blandford, R.D., & Königl, A. 1979, ApJ, 232, 34

Blandford, R.D., & Rees, M.J. 1978, in BL Lac Objects, ed. A.M. Wolfe (Univ. of Pittsburgh Press), 328

Blandford, R.D., & Znajek, R. 1977, MNRAS, 179, 433

Bregman, J.N., et al. 1990, ApJ, 352, 574

Brown, L.M.J., et al. 1989, ApJ, 340, 129

Burbidge, G.R., Jones, T.W., & O'Dell, S.L. 1974, ApJ, 193, 43

Celotti, A., Maraschi, L., & Treves, A. 1991, ApJ, 377, 403

Conway, J.E. 1993, in Sub-arcsecond Radio Astronomy, ed. R.J. Davies & R.S. Booth (Cambridge Univ. Press), in press

Cotton, W.D., & Spangler, S.R., ed. 1982, Low Frequency Variability of

Extragalactic Radio Sources (National Radio Astron. Obs.)
Courvoisier, T.J.-L., et al. 1987, A&A, 176, 197
Dent, W.A., & Balonek, T.J. 1980, Nature, 283, 747
Dermer, C.D., Schlickeiser, R., & Mastichiadis, A. 1992, A&A, 256, L27
Epstein, E.E., Fogarty, W.G., Mottmann, J., & Schneider, E. 1982, AJ, 87, 449
Fiedler, R.L., Pauls, T., Johnston, K.J., & Dennison, B. 1992, ApJ, submitted
Gabuzda, D.C., Cawthorne, T.V., Roberts, D.H., & Wardle, J.F.C. 1992, ApJ, 388, 40
Ghisellini, G., Maraschi, L., & Treves, A. 1985, A&A, 146, 204
Götz, M.M.A., Alef, W., Preuss, E., & Kellermann, K.I. 1987, A&A, 176, 171
Hardee, P.E. 1990, in Parsec-Scale Radio Jets, ed. J.A. Zensus & T.J. Pearson (Cambridge Univ. Press), 266
Hartman, R.C., et al. 1992, ApJ, 385, L1
Heeschen, D.S., Krichbaum, T., Schalinski, C.J., & Witzel, A. 1987, AJ, 94, 1493
Hufnagel, B.R., & Bregman, J.N. 1992, ApJ, 386, 473
Hughes, P.A., Aller, H.D., & Aller, M.F. 1985, ApJ 298, 301
Jones, T.W. 1982, BAAS, 14, 963 (abstract)
Kanbach, G., et al. 1992, IAU Circular no. 5431
Kawai, N., et al. 1991, ApJ, 382, 508
Königl, A. 1981, ApJ, 243, 700
Krichbaum, T.P., Quirrenbach, A., & Witzel, A. 1992, in Variability of Blazars, ed. E. Valtaoja & M. Valtonen (Cambridge Univ. Press), 331
Krichbaum, T.P., & Witzel, A. 1992, in Variability of Blazars, ed. E. Valtaoja & M. Valtonen (Cambridge Univ. Press), 205
Lovelace, R.V.E. 1976, Nature, 262, 649
Makino, F., et al. 1989, ApJ, 347, L9
Maraschi, L. 1992, in Variability of Blazars, ed. E. Valtaoja & M. Valtonen (Cambridge Univ. Press), 447
Maraschi, L., Ghisellini, G., & Celotti, A. 1992, ApJ, in press.
Marscher, A.P. 1980, ApJ, 235, 386
Marscher, A.P. 1988, ApJ, 334, 552
Marscher, A.P. 1990, in Parsec-Scale Radio Jets, ed. J.A. Zensus & T.J. Pearson (Cambridge Univ. Press), 236
Marscher, A.P. 1992, in Physics of Active Galactic Nuclei, ed. S.J. Wagner & W.J. Duschl (Heidelberg: Springer-Verlag), in press
Marscher, A.P., & Broderick, J.J. 1985, ApJ, 290, 735
Marscher, A.P., & Gear, W.K. 1985, ApJ, 298, 114
Marscher, A.P., Gear, W.K., & Travis, J.P. 1992, in Variability of Blazars, ed. E. Valtaoja & M. Valtonen (Cambridge Univ. Press), 85
Marscher, A.P., & Travis, J.P. 1991, in Variability of Active Galactic Nuclei, ed. H.R. Miller & P.J. Wiita (Cambridge Univ. Press), 153
Marscher, A.P., Zhang, Y.F., Shaffer, D.B., Aller, H.D., & Aller, M.F. 1991, ApJ, 371, 491
McBreen, B. 1979, A&A, 71, L19
McHardy, I.M., Marscher, A.P., Gear, W.K., Muxlow, T., Lehto, H.J., & Abraham, R.G. 1990, MNRAS, 246, 305
Melia, F., & Königl, A. 1989, ApJ, 340, 162
Michelson, P.F., et al. 1992, IAU Circular no. 5470
Mutel, R.L., Aller, H.D., & Phillips, R.B. 1981, Nature, 294, 236

O'Dell, S.L., et al. 1988, ApJ, 326, 668
Pauliny-Toth, I.I.K., Porcas, R.W., Zensus, J.A., Kellermann, K.I., Wu, S.Y., Nicolson, G.D., & Mantovani, F. 1987, Nature, 328, 778
Pauliny-Toth, I.I.K., Zensus, J.A., Cohen, M.H., Alberdi, A., & Schaal, R. 1990, in Parsec-Scale Radio Jets, ed. J.A. Zensus & T.J. Pearson (Cambridge Univ. Press), 55
Pearson, T.J., & Readhead, A.C.S. 1988, ApJ, 328, 114
Phinney, E.S. 1987, in Superluminal Radio Sources, ed. J.A. Zensus & T.J. Pearson (Cambridge Univ. Press), 301
Qian, S.J., Quirrenbach, A., Witzel, A., Krichbaum, T.P., Hummel, C.A., Zensus, J.A. 1991, A&A, 241, 15
Quirrenbach, A., et al. 1991, ApJ, 372, L71
Quirrenbach, A., Witzel, A., Krichbaum, T., Hummel, C.A., Alberdi, A., & Schalinski, C. 1989, Nature, 337, 442
Rantakyrö, F.T., Bååth, L.B., Pauliny-Toth, I.I.K., Matveyenko, L.I., & Unwin, S.C. 1992, A&A, 259, 8
Readhead, A.C.S., Cohen, M.H., Pearson, T.J., & Wilkinson, P.N. 1978, Nature, 276, 768
Reid, M.J., Biretta, J.A., Junor, W., Muxlow, T.W.B., & Spencer, R.E. 1989, ApJ, 336, 112
Reynolds, S.P. 1982, ApJ, 256, 13
Rickett, B.J., Coles, W.A., & Bourgois, G. 1984, A&A, 134, 390
Roberts, D.H., Wardle, J.F.C., Brown, L.F., Gabuzda, D.C., & Cawthorne, T.V. 1990, in Parsec-Scale Radio Jets, ed. J.A. Zensus & T.J. Pearson (Cambridge Univ. Press), 110
Shaffer, D.B., Marscher, A.P., Marcaide, J., & Romney, J.D. 1987, ApJ, 314, L1
Silanpää, A., & Takalo, L.O. 1992, in Variability of Blazars, ed. E. Valtaoja & M. Valtonen (Cambridge Univ. Press), 306
Tananbaum, H., et al. 1979, ApJ, 234, L9
Tang, G., Bartel, N., Ratner, M.I., Shapiro, I.I., Bååth, L.B., & Rönnäng, B. 1990, in Parsec-Scale Radio Jets, ed. J.A. Zensus & T.J. Pearson (Cambridge Univ. Press), 32
Unwin, S.C. 1990, in Parsec-Scale Radio Jets, ed. J.A. Zensus & T.J. Pearson (Cambridge Univ. Press), 13
Unwin, S.C., et al. 1985, ApJ, 289, 109
Unwin, S.C., & Wehrle, A.E. 1992, ApJ, in press
Venturi, T., et al. 1993, in Sub-arcsecond Radio Astronomy, ed. R.J. Davies & R.S. Booth (Cambridge Univ. Press), in press
Walker, R.C., Benson, J.M., & Unwin, S.C. 1987a, ApJ, 316, 547
Walker, R.C., Benson, J.M., & Unwin, S.C. 1987b, in Superluminal Radio Sources, ed. J.A. Zensus & T.J. Pearson (Cambridge Univ. Press), 48
Weekes, T.C. 1992, IAU Circular no. 5522
Wehrle, A.E., Cohen, M.H., Unwin, S.C., Aller, H.D., Aller, M.F., & Nicolson, G. 1992, ApJ, 391, 589
Wilkes, B.J., & Elvis, M. 1987, ApJ, 323, 243
Worrall, D.M., and Wilkes, B.J. 1990, ApJ, 360, 396
Zensus, J.A. 1990, in Parsec-Scale Radio Jets, ed. J.A. Zensus & T.J. Pearson (Cambridge Univ. Press), 28